Published in final edited form as:
J Comp Neurol. 2010 June 1; 518(11): 2090–2108. doi:10.1002/cne.22323.

Identifying the efferent projections of leptin-responsive neurons in the dorsomedial hypothalamus using a novel conditional tracing approach

Laurent Gautron[1,*], **Michael Lazarus**[2,*], **Michael M. Scott**[1], **Clifford B. Saper**[3], and **Joel K. Elmquist**[1]

[1]Departments of Internal Medicine and Pharmacology, Division of Hypothalamic Research, The University of Texas Southwestern Medical Center, 5323 Harry Hines Blvd, Dallas, Texas 75390-9077, Office: +1 214-648-6436, Fax Number: +1 214-648-5612

[2]Department of Molecular Behavioral Biology, Osaka Bioscience Institute, 6-2-4 Furuedai, Suita, Osaka 565-0874, Japan

[3]Department of Neurology, Beth Israel Deaconess Medical Center, and Program in Neuroscience, Harvard Medical School, Boston, MA, 02215

Abstract

Tracing the axonal projections of selected neurons is labor intensive and inherently limited by currently available neuroanatomical methods. We developed an adeno-associated virus (AAV) that can be used for efficiently tracing identified neuronal populations. The virus encodes a humanized *Renilla* Green Fluorescent Protein (hrGFP) which is transcriptionally silenced by a neo cassette flanked by LoxH/LoxP sites (AAV-lox-Stop-hrGFP). Thus, hrGFP is expressed only in neurons with Cre recombinase activity. To demonstrate the utility of this approach, the virus was injected unilaterally into the dorsomedial hypothalamus (DMH) of mice that express Cre in neurons expressing the leptin receptor. Animals with DMH injections showed robust hrGFP expression in DMH neurons, as visualized by its endogenous fluorescence or following immunolabeling. We found that hrGFP was expressed in approximately 1/3 to 1/2 of Cre-expressing neurons at the site of injection, but not in non-Cre-expressing neurons. The expression of GFP allowed us to identify the projection fields of DMH leptin-responsive neurons. Our results show hrGFP-positive axonal projections and terminals in the paraventricular nucleus of the hypothalamus, arcuate nucleus, preoptic area, bed nucleus of the stria terminalis, paraventricular thalamus, periaqueductal gray and precoeruleus. The aforementioned pattern of projections was similar to DMH projections determined by injections of biotinylated dextran amine in the mouse DMH. Interestingly, some hrGFP-positive terminals were seen contacting the ependymal layer of the 3rd and 4th ventricles. In summary, this approach is an effective tool to trace axonal projections of chemically identified neurons, including leptin-responsive neurons.

Keywords

Adeno-Associated Virus; Cre-Lox; Green Fluorescent Protein; Mouse

Correspondence should be addressed to JKE: Joel.Elmquist@UTSouthwestern.edu.
*contributed equally to this work.

Introduction

Identification of the neural pathways responsible for the metabolic and behavioral actions of leptin has become a major focus (e.g. Schwartz et al., 2000; Saper et al., 2002; van de Wall et al., 2008). Accordingly, our group and many others have found that leptin receptors are expressed in multiple brain sites, any number of which could mediate the varied actions of leptin (Mercer et al. 1996; Cheung et al. 1997; Fei et al. 1997; Elmquist et al. 1998b). The highest expression of leptin receptor is found in the hypothalamus within a distributed network of leptin-responsive neurons interconnected with several hypothalamic and extra-hypothalamic sites.

The basic connections of leptin-responsive neurons has begun to be deciphered by using neuroanatomical tract tracing combined with the assessment of leptin-induced gene expression. For example, we previously identified leptin-responsive neurons projecting from the dorsomedial hypothalamus (DMH) to the paraventricular hypothalamus (PVH) (Elmquist et al., 1998a), and also projecting from the arcuate nucleus (Arc) to the lateral hypothalamus (LH) (Elias et al., 1999) and the spinal cord (Elias et al., 1998).

Nevertheless, the vast majority of leptin-responsive neuron axonal projections have not been thoroughly investigated since the task is particularly challenging due to inherent technical difficulties. Indeed, the hypothalamus consists of a collection of small nuclei that are interconnected and send projections to the entire neuraxis, including an estimated 5,000 connections in rat (Bota and Swanson, 2007). Furthermore, systematic tracing of axonal projections from selected neurons using conventional neuroanatomical methods remains a difficult process. Briefly, tracing axonal projections from selected neurons can be achieved by stereotaxically injecting a retrograde tracer into a potential target site. Then, brain sections can be processed for the combined detection of the retrograde tracer with a marker that defines specifically the retrogradely-labeled neurons (for example, with a marker for leptin responsiveness). This step can be achieved by performing dual-label immunohistochemistry or immunohistochemistry combined with *in situ* hybridization. Hence, it is possible to evaluate whether or not the retrograde tracer and the selective marker colocalize within the same neurons. However, the systematic mapping of potential target sites requires repeating tract tracing for each brain site in different animals. Also, it is hard to confine retrograde tracers injections to small hypothalamic nuclei, and hence the adjacent structures are virtually always errantly injected. In summary, such approaches remain inherently difficult.

In order to circumvent such difficulties we developed a new approach based on Cre-LoxP technology for neural tracing of selected and identified neurons. We generated an adeno-associated virus (AAV) that encodes a humanized *Renilla* Green Fluorescent Protein (hrGFP) which is transcriptionally silenced by a neo cassette flanked by LoxH/LoxP sites (AAV-lox-Stop-hrGFP). The virus was stereotaxically-injected into the DMH of mice that express Cre under the control of the leptin receptor promoter (LepRb-Cre mice) (DeFalco et al., 2001; Scott et al., 2009). This delivery method has been previously used to induce gene expression in specific brain sites with minimal injury (Chamberlin et al., 1998). Consequently, animals with verified DMH injections showed robust hrGFP expression specifically in leptin-responsive neurons. Moreover, hrGFP was efficiently transported in axonal projections to brain sites known to be innervated by the DMH.

Materials and methods

Generation of conditional hrGFP-expressing AAV

For the generation of the AAV-lox-Stop-hrGFP vector plasmid, a loxH-Neo^R-loxP cassette derived by PCR from the pDisrupter2 plasmid (Zigman et al., 2005) was inserted between the EcoRI and SalI sites of the pAAV-MCS8 plasmid, kindly provided by the Harvard Viral Vector Core Laboratory (Richard Mulligan, director). This construct was further modified by blunt ligation of a BamHI/HindIII fragment from phrGFP-1 expression vector (Stratagene) into the XhoI site downstream of the loxP site. The AAV was generated by tripartite transfection (AAV-rep2/cap2 expression plasmid, adenovirus helper plasmid and AAV-lox-Stop-hrGFP vector plasmid) into 293A cells and purified by heparin column as previously described (Zolotukhin et al., 1999). The eluted virus was dialyzed against phosphate-buffered saline (PBS) and tittered by dot blot hybridization. A map of the construct is provided in Figure 1.

Animals

The LepRb-Cre mice express Cre from an IRES element inserted into the 3' untranslated region of the leptin receptor gene. Their genetic background is an admixture of C57Bl6/J and 129. The animals have been characterized carefully by our group and others (DeFalco et al., 2001; Scott et al., 2009). For instance, Cre expression in mice carrying 1 or 2 copies of the transgene allows efficient recombination in all leptin-responsive neurons and not in any other neurons. In order to visualize leptin-responsive neurons, we crossed the LepRb-Cre mice with reporter mice that express beta-galactosidase (β-gal) in a Cre-dependent manner as described by Scott and colleagues (2009). In the absence of Cre, a premature termination of the gene transcript results in no β-gal expression. In Cre-expressing neurons, the transcriptional termination sequence is excised allowing β-gal production from the ROSA26 locus in LepRb-expressing cells. C57Bl6/J mice purchased from the Jackson Laboratory were also used for anterograde tracing studies. Our mice were all males (~25 g) housed in a light-controlled (12 hours on/12 hours off; lights on at 7 a.m.) and temperature-controlled environment (21.5–22.5°C). The animals and procedures used were approved by University of Texas Southwestern Medical Center at Dallas Institutional Animal Care and Use Committees.

Brain surgery

LepRb-Cre (n=13) and LepRb-Cre-LacZ (n= 10) mice were stereotaxically injected with AAV-lox-stop-hrGFP following previously described procedures (Chamberlin et al., 1998). Briefly, mice were anesthetized with Ketamine HCl/Xylazine HCl (80/12 mg/kg, i.p.) and restrained in a Kopf stereotaxic apparatus. Then, a small hole was drilled into the skull under aseptic conditions. A glass micropipette connected to an air pressure injector system was positioned via the stereotaxic manipulator. The AAV-lox-Stop-hrGFP was administered slowly (~250 nl, 7.6×10^{12} particles/ml) into the DMH (−1.88 mm from bregma, ±0.43 mm lateral, −5.3mm from the surface of the skull). Coordinates were chosen to be centered into the ventral part of the DMH. In a pilot study, we have determined that 250nl is the optimal volume to obtain significant hrGFP expression in the DMH without spreading to the adjacent hypothalamic nuclei (not shown). C57Bl/6 mice (n=10) were similarly injected with ~50–100nl of the anterograde tracer biotin dextran amine (BDA) (5% in water; Molecular Probes; 10,000 MW; Cat#D1956, lot#50509A). After injection, the micropipette was removed and the incision was closed with surgical staples.

AAV-injected mice were allowed to survive 4 weeks post-surgery. It has been demonstrated that the AAV-mediated delivery of GFP expression is identical from 2 weeks up to 12 weeks post-surgery (Chamberlin et al., 1998). Therefore, we anticipated that the survival time point

would have little influence on our results. Mice injected with BDA survived between 5 to 7 days, which is a commonly used period for anterograde tracing using BDA 10,000 in rats and mice (Chou et al., 2002; Schuz et al., 2006; Kaneda et al., 2008; Kaufling et al., 2009).

Perfusion

On the day of sacrifice, mice were deeply anesthetized with chloral hydrate (500 mg/kg, ip), and then were perfused transcardially with 0.9% saline followed by 10% formalin (Sigma). The brain was removed, post-fixed 2 hours, and submerged in 20% sucrose overnight at 4°C. Coronal sections were cut at 25μm using a freezing microtome (1:5 series). Sections were collected in 0.1 M phosphate buffered saline (PBS) (pH 7.4), transferred in a cryoprotectant solution and stored at −20°C.

Antibodies characterization

The 2 primary antisera used in this study are commercially available, and their key features are summarized in Table 1.

1- Rabbit anti-hrGFP polyclonal antiserum (Stratagene). The manufacturer analyzed the antibody by Western blot using transfected cells. Western blot analysis produced a single band of 32.5kDa corresponding to hrGFP (manufacturer's information), and demonstrated that the antiserum does not show cross-reactivity with eGFP. Yang and colleagues (2009) used this antiserum to detect AAV-mediated expression of hrGFP in the rat brain and in 293A infected cells. The staining that we obtained using this antibody was cytoplasmic and was present in both cell bodies and projections. Immunoreactivity was absent in brain sections from wild-type mice (not shown). Importantly, hrGFP-expressing neurons showed bright endogenous fluorescence that is directly comparable to the immunostaining obtained on adjacent sections (Fig. 2).

2- Chicken anti-beta-galactosidase (β-gal) polyclonal antiserum (Abcam). The manufacturer has previously analyzed the antibody specificity by ELISA against 1μg of purified β-gal. Furthermore, the antibody has been shown to detect β-gal in the nervous system of different transgenic mice expressing LacZ under the control of specific promoters such as melanopsin, Sall3 or leptin receptor promoters (Baver et al., 2008; Harrison et al., 2008; Scott et al., 2009). In our samples, the antiserum produced moderate cytoplasmic staining and bright punctate labeling in the cell nucleus. The cellular and anatomic distribution of β-gal immunoreactivity in our samples was directly comparable to that previously obtained with the same antiserum in LepRb-Cre-LacZ mice (Scott et al., 2009). Lastly, the antiserum produces no staining in wild-type animals (not shown).

Histology

Indirect immunofluorescence technique—After washing in PBS, brain sections were incubated overnight at room temperature in a hrGFP rabbit primary antiserum (Stratagene; 1:30,000; see Table 1) in 3% normal donkey serum (Jackson ImmunoResearch Laboratories Inc., West Grove, PA) with 0.25% Triton X-100 in PBS (PBT). After washing in PBS, sections were incubated in Alexa 488-conjugated anti-rabbit secondary antibody (Invitrogen; cat#A11039; lot#57542A; 1:1,000) for 1 hour at room temperature. The labeling obtained after using the immunofluorescence technique was directly comparable to the endogenous fluorescence viewed on adjacent sections (Fig. 2).

Indirect immunoperoxidase technique—After washing in PBS, brain sections were pretreated with 0.3% hydrogen peroxide in PBS for 15 min at room temperature. Sections were incubated overnight in rabbit primary antiserum in PBT (1:50,000) followed by biotinylated donkey anti-rabbit (Jackson Immunoresearch; cat#711065152; lot#81161), then

incubated in a solution of ABC (Vectastain Elite ABC Kit; Vector Laboratories, Burlingame, CA; 1:1,000) dissolved in PBS for 1 hour. After washing in PBS, the sections were incubated in a solution of 0.04% diaminobenzidine tetrahydrochloride (DAB, Sigma), 0.01% nickel ammonium sulfate (Fisher Scientific), 0.01% cobalt chloride (Fisher Scientific), and 0.01% hydrogen peroxide (Aldrich). The same technique was used to detect BDA. Briefly, sections were pre-treated with 0.3% hydrogen peroxide in PBS, followed by an overnight incubation in a solution of ABC in PBT without normal serum. After washing in PBS, the tissue was labeled with DAB exactly as described above.

Double immunostaining for β-gal and hrGFP was also carried out. Sections were incubated overnight at room temperature in a mixture of anti-β-gal and anti-hrGFP primary antibodies (see Table 1) in PBT with donkey normal serum. On the next day, sections were incubated in anti-chicken biotinylated secondary antibody (Jackson Immunoresearch; Cat#703065155; lot#78100) followed by Alexa 594-conjugated streptavin (Invitrogen; Cat#532356; lot#459559). After several washes, the tissue was labeled for hrGFP using the indirect immunofluorescent technique exactly as described above. It resulted in the fluorescent labeling of hrGFP-positive neurons including cell bodies and axons in green, and of β-gal-positive neurons in red.

Immunofluorescent detection was used to perform double immunohistochemical detection of hrGFP and β-gal and to generate optical sections of axon terminals as represented in Figures 4, 6, 8 and 9. Immunoperoxidase detection was carried out in order to map axons terminals and generate line drawings as represented in Figures 3, 7, 10, 11 and 12.

Fluorescently-labeled sections (hrGFP alone or combined with β-gal) were mounted on gelatin-coated slides, air-dried and coverslipped with vectashield mounting medium containing DAPI (Vector laboratories, Burlingame, CA; H-1500). DAB-labeled sections (hrGFP or BDA) were mounted on gelatin-coated slides, air-dried, dehydrated in graded ethanols, cleared in xylenes, and coverslipped with Permaslip (Alban Scientific).

Microscopy and production of digital images

Endogenous fluorescence and DAB staining were viewed using a Zeiss microscope (Axioskop2) using fluorescent and brightfield optics respectively. Digital images were captured using a digital camera (Axiocam) attached to the microscope and a desktop computer running the Axiovision 3.1 software. High resolution fluorescent images of hrGFP represented in Figures 2, 4, 6, 8 and 9 were generated using stacks of optical sections (between 5 to 8 sections covering a thickness of ~10μm) obtained with a Zeiss microscope (Imager ZI) attached to the Apotome system. Images were captured with a digital camera (Axiocam) attached to the microscope and a desktop computer running Axiovision 4.5.

We sought to estimate the overall sensitivity of our method by counting neurons being both β-gal- and hrGFP-positive. A cell was considered doubly-labeled only when the shape of β-gal- and GFP-positive profiles properly corresponded. Cell counts were performed using a 10x objective and a fluorescent microscope on one selected section per level at 3 different rostro-caudal levels of the DMH in a total of 4 cases (Fig. 5). Data are presented as ratio of hrGFP/β-gal-positive cells in the DMH of each individual case. Importantly, we expected variability in our injections and therefore our counts are only meant to provide relative data but not accurate counts of absolute cell numbers. The data were not corrected for double counting, nor was the stereological technique used since the cell size and section thickness did not vary between animals.

We provided qualitative estimates of hrGFP- and BDA-positive fibers considering the density of positive fibers and terminals (Table 2). The relative densities of fibers are given

per brain region independently of its surface. Densities were subjectively determined by visual inspection of brain sections as follows: + + + +, very high; + + +, high; + +, moderate; +, low; +/−, not consistently seen; −, absent. Once again, these data are inherently qualitative.

Drawings were generated using a camera lucida-equipped microscope, digitalized and incorporated in the software Adobe Illustrator CS2. The image editing software Adobe Photoshop CS2 was used to combine drawings and digital images into plates. The contrast and brightness of images were adjusted. Red-green fluorescence images were converted to magenta-green for the readers who are color blind. We used the Franklin and Paxinos mouse brain atlas (1997) as a reference for anatomical landmarks and abbreviations.

Results

Conditional expression of hrGFP

We initially visualized hrGFP endogenous fluorescence under fluorescence optics. As a result, we observed DMH hrGFP expression in 4 out of 13 cases. Indeed, stereotaxic microinjections in small nuclei inherently resulted in a high percentage of missed injections centered outside of the hypothalamus. However, the “missed” injections, outside the DMH in non-leptin receptor-expressing nuclei, serve as an anatomic control and demonstrate that the expression of hrGFP is completely prevented in the absence of Cre recombinase. We observed bright endogenous fluorescence within the DMH in clustered neuronal cell bodies and their proximal dendrites (Fig. 2A, B). GFP-positive neurons were found mostly in the ventral DMH but carefully avoided the compact part of the DMH (Fig. 2B), which strongly suggests that the recombination occurred only in leptin-responsive neurons as expected. Immunohistochemistry was also performed on adjacent series of sections using either fluorescent (Fig. 2C) or peroxidase-conjugated secondary antibodies (Fig. 2D). We observed a similar distribution pattern of hrGFP after immunohistochemistry (Fig. 2C,D).

The anatomical distribution of hrGFP expression within the DMH was analyzed in the 4 successful cases (Fig. 3). Cases 5, 6 and 65 showed hrGFP expression almost exclusively centered in the DMH including its caudoventral part and to a lesser extent in its rostral and dorsal parts. Case 18 showed additional expression outside of the DMH in neurons located in the Arc and ventral premammillary nucleus (PMV).

Evaluation of the specificity and sensitivity of hrGFP expression

In order to confirm the utility of our method, we verified that hrGFP was expressed only in leptin responsive neurons (specificity) and we estimated the proportion of leptin responsive neurons expressing hrGFP (sensitivity). Injections were repeated in LepRb-Cre-LacZ mice in which LepRb-expressing neurons can be directly visualized following β-gal immunolabeling (Scott et al., 2009). As shown in Figure 4, β-gal was observed in the DMH, VMH (ventromedial nucleus of the hypothalamus), Arc and LH (Fig. 4A). Our injections resulted in hrGFP expression concentrating in the ventral DMH ipsilateral to the site of injection (Fig. 4B). At higher magnification, hrGFP systematically colocalized with β-gal (Fig. 4C, D), which indicate that hrGFP expression occurred exclusively in Cre-expressing neurons. However, singly labeled β-gal-positive neurons were also observed (Fig. 4C, D). We obtained 4 out of 10 cases with DMH hrGFP expression. Of note, the distribution and number of hrGFP neurons was comparable to that seen in our LepRb-Cre mice previous cases (Fig. 3). Other cases showed expression centered in the LH or no expression (not shown).The proportion of β-gal-positive neurons showing hrGFP immunoreactivity varied across anatomical levels and animals (Fig. 5). The ventral part of the medial DMH, which corresponds to our site of injection, contained the largest proportion of hrGFP-positive

neurons. At this anatomical level, hrGFP-positive neurons roughly represented between 1/3 and 1/2 of all β-gal-positive neurons (Figure 5). In its more rostral and posterior parts, the DMH showed variable expression and smaller numbers of hrGFP-positive neurons (Fig. 5). The aforementioned results demonstrate the overall sensitivity of our method near the site of injection, but also show a limited spread of transfection.

Mapping of leptin-responsive neuron axonal projections

Axons positive for hrGFP were observed in the PVH (Fig. 6A, B), a site known to be innervated by DMH leptin-responsive neurons (Elmquist et al., 1998a). At higher magnification, we could identify fibers of passage near the PVH (Fig. 6C). Inside of the PVH itself, fibers with complex ramifications associated with clusters of boutons were often observed (Fig. 6D). Those fibers are likely to be axon terminals circling target neurons. These preliminary observations indicate that hrGFP acts as an excellent anterograde tracer, allowing the visualization of axons and terminals.

Despite the fact that our stereotaxic injections resulted in variable hrGFP expression, the full projection fields of leptin-responsive neurons was very comparable across injected-animals. Hence, we observed an identical pattern of projections in all 7 cases (3 LepRb-Cre and 4 LepRb-Cre-LacZ) with only small variations in the densities of hrGFP-positive fibers (Table 2). Case #18 was not included because it comprised significant hrGFP in leptin-sensitive neurons outside of the DMH. Figure 7 illustrates the typical distribution pattern of hrGFP-positive fibers throughout the brain of case #65 (LepRb-Cre), while Figure 8 shows representative photomicrographs of selected target sites from case #8 (LepRb-Cre-LacZ). Projections were seen in the entire rostro-caudal extension of the Arc and PVH which were particularly enriched with boutons (Fig. 7; 8D, E). We also found significant projections in undifferentiated parts of the preoptic area and in the bed nucleus of stria terminalis (Fig. 7; 8C), supraoptic nucleus (Fig. 7), lateral septum (Fig. 7; 8A), paraventricular thalamus (Fig. 7; 8B), periacqueductal gray (mostly its ventrolateral part) (Fig. 7; 8F, G) and the precoeruleus (Fig. 7; 8H). Smaller projections consisting of passing fibers were seen in the lateral hypothalamus, mammillary nuclei, and dorsal raphé (Fig. 7). Although most fibers were observed in the side ipsilateral to the site of injection, a few fibers were also seen in the contralateral Arc, PVH, preoptic area, and central gray. In case 18 only, we found fibers in brain sites not connected to the DMH which likely originate from transduced neurons in the Arc and PMV (not shown). Interestingly, fibers were seen traveling closely along the ependymal layer at the level of the 3rd and 4th ventricles near the PVH, paraventricular thalamus and periacqueductal gray. In several occasions, these fibers traveled through the ependymal layer itself and seemingly contacted the cerebrospinal fluid (Fig. 9).

Comparison with generic DMH projections in the mouse brain

Although DMH efferent projections have already been described in rats (Ter Horst and Luiten, 1986; Thompson et al., 1996), we sought to determine whether or not they are identical in mice and qualitatively comparable to leptin-sensitive neuron efferent projections. We obtained 4 cases with BDA injections centered in the DMH (Figure 10). Our injections were large and encompassed the DMH in its entire rostro-caudal extension. Case #1 is used as an example in Figure 11 because it comprised the entire DMH with minimal spread outside of its boundaries.

As a result, the pattern of projections obtained following BDA injections was virtually identical to that described in rats by Thompson and colleagues (1996). Briefly, heavy projections were seen in the PVH, undifferentiated parts of the preoptic, and the DMH itself (Fig. 11). Moderate to abundant projections were also found in the bed nucleus of stria terminalis, lateral septum, lateral hypothalamus, paraventricular thalamus, periacqueductal

gray (Fig. 11). Smaller projections were seen in the supraoptic nucleus and precoeruleus (Fig. 11). High magnification photomicrographs illustrate the observed heavy, moderate and light innervations of the PVH (Fig. 12A), periacqueductal gray (Fig. 12B) and Arc (Fig. 12C) respectively. Additional target sites were seen in mice with larger injection sites including the raphe pallidus, subiculum, and striatum (not shown). Terminals in the aforementioned structures likely result from BDA deposited above the DMH and along the tract through the thalamus. For example, it is known that the raphe pallidus does receive heavy projections from a cluster of neurons residing above the DMH (Hosoya et al., 1987; Hermann et al., 1997; Yoshida et al., 2009). Based on a qualitative comparison of the distribution pattern of fibers (Table 2), we reached the conclusion that leptin sensitive neurons in the mouse DMH show a directly comparable pattern of projections to that of generic DMH projections with only a difference in the densities of innervation. One discrepancy, however, relates to the innervation of the Arc (Table 2). Whereas it was only lightly innervated by BDA-positive fibers (Fig. 12), it received relatively abundant innervation from hrGFP-positive fibers (Fig. 6, 7).

Similarly to hrGFP fibers, it appears that BDA-positive fibers contacted the ventricles. For instance, BDA-positive fibers seemingly traveling through the ependymal layer at the level of the aqueduct are shown in Figure 12D.

Discussion

In the current series of studies, we designed a virus (AAV-lox-stop-hrGFP) that can be used for efficiently tracing the cell bodies and axons of selected neurons. To demonstrate the utility of this approach, the virus was injected unilaterally into the DMH of mice that express Cre in neurons expressing leptin receptors. Mice with successful injections showed hrGFP expression only in leptin-responsive neurons of the DMH. This limited population of neurons sends projections terminating in several brain structures involved in the control of energy homeostasis and daily rhythms.

Technical considerations

Previous studies have established in great detail the usefulness of GFP labeling of axons, dendrites and presynaptic compartments using two-photons and electron microscopy (Campbell et al., 2009; Knott et al., 2009). New approaches for neural tracing of selected neurons have been recently developed based on the conditional expression of GFP. Originally, DeFalco and colleagues (2001) performed a virus-assisted mapping of leptin receptor-expressing neuronal afferent projections. Their method involved multisynaptic infection of afferent neurons specifically innervating leptin-sensitive neurons in the Arc using a pseudorabies virus. Another study used a mouse line expressing a fusion protein between the C-terminal fragment of tetanus toxin and GFP in orexin neurons (Sakurai et al., 2005), resulting in the labeling of neurons projecting to orexin neurons. Overall, these methods differ from our own both in terms of applicability (short-term vs. long-term) and/or purpose (afferents vs efferents).

The method described in this study presents unique advantages in comparison to conventional methods. First of all, it allows the conditional expression of hrGFP only in neurons that express Cre recombinase and not in any other cells. The hrGFP is efficiently transported to axon terminals and is easily detected either by immunohistochemical means or by visualizing its endogenous fluorescence. Therefore, our method allows the tracing of axons terminals in multiple target sites in the same brain. Also, AAV-mediated gene delivery provides continuous expression of hrGFP in neurons, which makes our method compatible with a variety of long-term neurobiological experiments. Recently, Myers and colleagues used an approach very similar to ours to label LepRb-expressing neurons in the

lateral hypothalamus and ventral premammillary nucleus using an adenovirus-Stop-Lox-GFP (Leshan et al., 2009; Leinninger et al., 2009). One difference with our study is the use of an adenovirus over an AAV to deliver GFP expression. Although AAVs are generally thought to be less immunogenic than adenoviruses, in fact, both types of vectors have been shown to procure lasting expression (of at least 2 months) with minimal inflammatory responses when injected at low dose into the brain parenchyma (Lowenstein et al., 2007). Yet the sensitivity and specificity of the adenovirus-Stop-Lox-GFP employed in earlier studies remains to be tested.

Despite these potential benefits, the success of our method requires the availability of reliable mouse models. Indeed, ectopic or leaking Cre expression may result in false positive results. Therefore, investigators who wish to use our method must verify in preliminary experiments whether or not the hrGFP expression is restricted to Cre-expressing neurons. For example, we verified that hrGFP expression perfectly coincided with β-gal expression. Those data indicated that Cre-mediated recombination occurred only in leptin-responsive neurons which are also Cre-expressing neurons. Another potential problem arises from the fact that the recombination occurred only in a restricted number of Cre-expressing neurons. For instance, while we observed satisfying hrGFP expression near the site of injection in the ventral DMH in approximately 1/3 to 1/2 of Cre-expressing neurons, a relatively small number of neurons were transduced in the rostral and caudal portions of the DMH. The aforementioned problem is not specific to our method but is inherent of most tracing studies which often result in undesired spread of tracers or variable sites of deposit. In fact, results obtained from differently positioned injections sites serve as anatomical controls and, in that respect, our method is not an exception. Also, AAV serotype 10 has been very recently used to achieve enhanced and widespread transduction of neurons as compared to AAV serotype 2 used in our study. Given those restrictions, our data remain inherently qualitative. Successful results rely on the concentration of the employed AAV as well (Chamberlin et al., 1998). For all these reasons, it is required to empirically the optimal volume and serotype of AAV to be injected in each Cre model and each potential site of injection for each batch of virus.

Despite some limitations, we obtained reliable hrGFP expression and an identical pattern of projections in several animals. The projection fields that we identified were widespread and directly comparable to that of standard methods identifying DMH projections. This indicates that leptin-responsive neurons in the DMH do not have preferential sites of innervation. Nonetheless, hrGFP immunoreactivity in the Arc was constantly more abundant than BDA immunoreactivity. This apparent discrepancy can be explained by the fact that hrGFP is continuously produced and transported to terminals, whereas conventional tracers such as BDA are present in a fixed amount. Nonetheless, this finding suggests that the innervation of the Arc originating from the DMH, although limited, probably exclusively consists of leptin-sensitive neurons.

Comparison with known DMH projections

The pattern of axonal projections originating from the DMH has previously been systematically investigated in rats using PHA-L injections (Ter Horst and Luiten, 1986; Thompson et al., 1996). These two studies reported a comparable pattern of projections to numerous intrahypothalamic, preoptic, limbic and midbrain sites. However, there are a few differences between the two studies. For example, Ter Horst and Luiten (1986) showed projections to the cortex, amygdala, circumventricular organs and ventral medulla that were not observed by Thompson and colleagues (1996). The reason for this discrepancy may be explained by the large injection sites in the first study which extended to the anterior hypothalamic nucleus and the lateral hypothalamus. Our own data demonstrate that mice

have a pattern of DMH projections identical to that described in rats (Thompson et al., 1996).

DMH neurons send prominent projections to the PVH (Ter Horst and Luiten, 1985; Thompson et al., 1996). Previously, our group has shown that some leptin-responsive neurons in the DMH send projections to the PVH (Elmquist et al., 1998a). However, whether or not leptin-responsive neurons in the DMH were connected exclusively to the PVH or to the full range of brain sites connected to the DMH remained unknown. The current data demonstrate that these neurons innervate a pattern of brain sites very similar to that seen after PHA-L injections in rats (Thompson et al., 1996) and BDA injections in mice. Such an observation further validates the reliability of our method and suggests that leptin-responsive neurons do not innervate exclusively the PVH but many brain sites innervated by the DMH. The current work also shows that leptin-responsive neurons in the DMH send projections to the Arc. Interestingly, DeFalco and colleagues (2001) had previously shown that the leptin-responsive neurons that reside in the Arc receive important innervations from the DMH. Together, our observations suggest that leptin-responsive neurons in the DMH and the Arc may have reciprocal projections.

Functional considerations

Remarkably, little is known regarding the role of leptin receptor in the DMH. Briefly, the administration of leptin activates STAT3 and induces a robust expression of c-fos and socs-3 in a cluster of neurons localized in the caudoventral DMH (Elmquist et al., 1997; Bjorbaek et al., 1998; Elias et al., 2000; Hubschle et al., 2001). However, the neurochemical identity of DMH leptin-responsive neurons remains unknown. Although early lesion studies have established the DMH as important in the homeostatic regulation of feeding and metabolism (Bernardis and Bellinger, 2002), it is only recently that the DMH has been found to be critical for the normal control of daily rhythms of a variety of physiological parameters including corticosterone secretion, body temperature, sleep and locomotor activity (Chou et al., 2003; Gooley et al., 2006). Notably, leptin signaling in the brain was found to exert profound effects on the regulation of corticosterone levels, body temperature and sleep (Pelleymounter et al., 1995; Cohen et al., 2001; Laposky et al., 2008). Moreover, we found that leptin- responsive neurons in the DMH innervate brain sites important in the control of these physiological parameters such as the PVH, preoptic area and precoeruleus. Therefore, it is possible that leptin signaling in the DMH regulates corticosterone secretion, body temperature and arousal. Also, leptin-responsive neurons densely innervate the Arc which is a site required for leptin action on glucose homeostasis and/or locomotor activity (Coppari et al., 2005). Thus, it is tempting to suggest that DMH leptin responsive neurons contribute to the coordinated regulation of glucose homeostasis and/or locomotor activity in response to leptin. Further experiments are needed to identify the role of leptin receptors expression in the DMH.

Another intriguing observation was made of the close association of axonal projections with the ependymal layer bordering the third ventricle and the aqueduct. It has been reported that subsets of neurons innervate the ependymal layer and/or contact the cerebrospinal fluid. For instance, cholera-toxin B injected into the ventricular system backfilled axons in the ependymal layer and neuronal cell bodies located mostly in the dorsal raphé but also scattered neurons in the hypothalamus (Mikkelsen et al., 1997). Consequently, it is plausible that some leptin responsive neurons innervate the ependymal layer and occasionally contact and sample the cerebrospinal fluid. The significance of such an observation is unclear but it is possible that those neurons release into the cerebrospinal fluid a substance with neuromodulatory functions. Alternatively, those neurons may sense a factor circulating in the cerebrospinal fluid, perhaps leptin itself.

Conclusion

In conclusion, the current data show that it is possible to efficiently selectively trace identified neuronal populations using conditional hrGFP expression. Specifically, our study reveals that leptin-responsive neurons in the DMH innervate several target sites, and thus may modulate a variety of physiological functions in response to leptin.

Acknowledgments

Funded by:

US Public Health Service grants NS33987 (M.L. and C.B.S.), DK53301, MH61583 (J. K. E.) and the American Diabetes Association 1-07-RA-41 (L.G. and J.K.E.), and Cores 1PL1DK081182 and 1UL1RR024923 (J.K.E).

We are grateful to Dr. Jeffrey Friedman (Rockfeller University) for providing us with LepRb-Cre mice.

Literature Cited

Baver SB, Pickard GE, Sollars PJ, Pickard GE. Two types of melanopsin retinal ganglion cell differentially innervate the hypothalamic suprachiasmatic nucleus and the olivary pretectal nucleus. Eur J Neurosci. 2008; 27(7):1763–1770. [PubMed: 18371076]

Bellinger LL, Bernardis LL. The dorsomedial hypothalamic nucleus and its role in ingestive behavior and body weight regulation: lessons learned from lesioning studies. Physiol Behav. 2002; 76(3): 431–442. [PubMed: 12117580]

Bjørbaek C, Elmquist JK, Frantz JD, Shoelson SE, Flier JS. Identification of SOCS-3 as a potential mediator of central leptin resistance. Mol Cell. 1998; 1(4):619–625. [PubMed: 9660946]

Bota M, Swanson LW. The neuron classification problem. Brain Res Rev. 2007; 56(1):79–88. [PubMed: 17582506]

Campbell RE, Gaidamaka G, Han SK, Herbison AE. Dendro-dendritic bundling and shared synapses between gonadotropin-releasing hormone neurons. Proc Natl Acad Sci U S A. 2009; 106(26): 10835–10840. [PubMed: 19541658]

Chamberlin NL, Du B, de Lacalle S, Saper CB. Recombinant adeno-associated virus vector: use for transgene expression and anterograde tract tracing in the CNS. Brain Res. 1998; 793(1–2):169–175. [PubMed: 9630611]

Cheung CC, Clifton DK, Steiner RA. Proopiomelanocortin neurons are direct targets for leptin in the hypothalamus. Endocrinology. 1997; 138(10):4489–4492. [PubMed: 9322969]

Chou TC, Scammell TE, Gooley JJ, Gaus SE, Saper CB, Lu J. Critical role of dorsomedial hypothalamic nucleus in a wide range of behavioral circadian rhythms. J Neurosci. 2003; 23(33): 10691–1702. [PubMed: 14627654]

Cohen P, Zhao C, Cai X, Montez JM, Rohani SC, Feinstein P, Mombaerts P, Friedman JM. Selective deletion of leptin receptor in neurons leads to obesity. J Clin Invest. 2001; 108(8):1113–1121. [PubMed: 11602618]

Coppari R, Ichinose M, Lee CE, Pullen AE, Kenny CD, McGovern RA, Tang V, Liu SM, Ludwig T, Chua SC Jr, Lowell BB, Elmquist JK. The hypothalamic arcuate nucleus: a key site for mediating leptin's effects on glucose homeostasis and locomotor activity. Cell Metab. 2005; (1):63–72. [PubMed: 16054045]

DeFalco J, Tomishima M, Liu H, Zhao C, Cai X, Marth JD, Enquist L, Friedman JM. Virus-assisted mapping of neural inputs to a feeding center in the hypothalamus. Science. 2001; 291(5513):2608–2613. [PubMed: 11283374]

Elias CF, Lee C, Kelly J, Aschkenasi C, Ahima RS, Couceyro PR, Kuhar MJ, Saper CB, Elmquist JK. Leptin activates hypothalamic CART neurons projecting to the spinal cord. Neuron. 1998; 21(6): 1375–1785. [PubMed: 9883730]

Elias CF, Aschkenasi C, Lee C, Kelly J, Ahima RS, Bjorbaek C, Flier JS, Saper CB, Elmquist JK. Leptin differentially regulates NPY and POMC neurons projecting to the lateral hypothalamic area. Neuron. 1999; 23(4):775–786. [PubMed: 10482243]

Elias CF, Kelly JF, Lee CE, Ahima RS, Drucker DJ, Saper CB, Elmquist JK. Chemical characterization of leptin-activated neurons in the rat brain. J Comp Neurol. 2000; 423(2):261–281. [PubMed: 10867658]

Elmquist JK, Ahima RS, Maratos-Flier E, Flier JS, Saper CB. Leptin activates neurons in ventrobasal hypothalamus and brainstem. Endocrinology. 1997; 138(2):839–842. [PubMed: 9003024]

Elmquist JK, Ahima RS, Elias CF, Flier JS, Saper CB. Leptin activates distinct projections from the dorsomedial and ventromedial hypothalamic nuclei. Proc Natl Acad Sci U S A. 1998a; 95(2):741–746. [PubMed: 9435263]

Elmquist JK, Bjørbaek C, Ahima RS, Flier JS, Saper CB. Distributions of leptin receptor mRNA isoforms in the rat brain. J Comp Neurol. 1998b; 395(4):535–547. [PubMed: 9619505]

Fei H, Okano HJ, Li C, Lee GH, Zhao C, Darnell R, Friedman JM. Anatomic localization of alternatively spliced leptin receptors (Ob-R) in mouse brain and other tissues. Proc Natl Acad Sci U S A. 1997; 94(13):7001–7005. [PubMed: 9192681]

Franklin, KBJ.; Paxinos, G. The mouse brain in stereotaxic coordinates. San Diego: Academic Press; 1997.

Gooley JJ, Schomer A, Saper CB. The dorsomedial hypothalamic nucleus is critical for the expression of food-entrainable circadian rhythms. Nat Neurosci. 2006; 9(3):398–407. [PubMed: 16491082]

Harrison SJ, Parrish M, Monaghan AP. Sall3 is required for the terminal maturation of olfactory glomerular interneurons. J Comp Neurol. 2008; 507(5):1780–1794. [PubMed: 18260139]

Hermann DM, Luppi PH, Peyron C, Hinckel P, Jouvet M. Afferent projections to the rat nuclei raphe magnus, raphe pallidus and reticularis gigantocellularis pars alpha demonstrated by iontophoretic application of choleratoxin (subunit b). J Chem Neuroanat. 1997; 13(1):1–21. [PubMed: 9271192]

Hosoya Y, Ito R, Kohno K. The topographical organization of neurons in the dorsal hypothalamic area that project to the spinal cord or to the nucleus raphé pallidus in the rat. Exp Brain Res. 1987; 66(3):500–506. [PubMed: 3609196]

Hübschle T, Thom E, Watson A, Roth J, Klaus S, Meyerhof W. Leptin-induced nuclear translocation of STAT3 immunoreactivity in hypothalamic nuclei involved in body weight regulation. J Neurosci. 2001; 21(7):2413–2424. [PubMed: 11264315]

Kaneda K, Isa K, Yanagawa Y, Isa T. Nigral inhibition of GABAergic neurons in mouse superior colliculus. J Neurosci. 2008; 28(43):11071–11078. [PubMed: 18945914]

Kaufling J, Veinante P, Pawlowski SA, Freund-Mercier MJ, Barrot M. Afferents to the GABAergic tail of the ventral tegmental area in the rat. J Comp Neurol. 2009; 513(6):597–621. [PubMed: 19235223]

Knott GW, Holtmaat A, Trachtenberg JT, Svoboda K, Welker E. A protocol for preparing GFP-labeled neurons previously imaged in vivo and in slice preparations for light and electron microscopic analysis. Nat Protoc. 2009; 4(8):1145–1156. [PubMed: 19617886]

Laposky AD, Bradley MA, Williams DL, Bass J, Turek FW. Sleep-wake regulation is altered in leptin resistant (db/db) genetically obese and diabetic mice. Am J Physiol Regul Integr Comp Physiol. 2008; 295(6):R2059–R2066. [PubMed: 18843095]

Leinninger GM, Jo YH, Leshan RL, Louis GW, Yang H, Barrera JG, Wilson H, Opland DM, Faouzi MA, Gong Y, Jones JC, Rhodes CJ, Chua S Jr, Diano S, Horvath TL, Seeley RJ, Becker JB, Münzberg H, Myers MG Jr. Leptin acts via leptin receptor-expressing lateral hypothalamic neurons to modulate the mesolimbic dopamine system and suppress feeding. Cell Metab. 2009; 10(2):89–98. [PubMed: 19656487]

Leshan RL, Louis GW, Jo YH, Rhodes CJ, Münzberg H, Myers MG Jr. Direct innervation of GnRH neurons by metabolic- and sexual odorant-sensing leptin receptor neurons in the hypothalamic ventral premammillary nucleus. J Neurosci. 2008; 29(10):3138–3147. [PubMed: 19279251]

Lowenstein PR, Mandel RJ, Xiong WD, Kroeger K, Castro MG. Immune responses to adenovirus and adeno-associated vectors used for gene therapy of brain diseases: the role of immunological synapses in understanding the cell biology of neuroimmune interactions. Curr Gene Ther. 2007; 7(5):347–360. [PubMed: 17979681]

Mercer JG, Hoggard N, Williams LM, Lawrence CB, Hannah LT, Trayhurn P. Localization of leptin receptor mRNA and the long form splice variant (Ob-Rb) in mouse hypothalamus and adjacent brain regions by in situ hybridization. FEBS Lett. 1996; 387(2–3):113–116. [PubMed: 8674530]

Mikkelsen JD, Hay-Schmidt A, Larsen PJ. Central innervation of the rat ependyma and subcommissural organ with special reference to ascending serotoninergic projections from the raphe nuclei. J Comp Neurol. 1997; 384(4):556–568. [PubMed: 9259489]

Münzberg H, Huo L, Nillni EA, Hollenberg AN, Bjørbaek C. Role of signal transducer and activator of transcription 3 in regulation of hypothalamic proopiomelanocortin gene expression by leptin. Endocrinology. 2003; 144(5):2121–2131. [PubMed: 12697721]

Pelleymounter MA, Cullen MJ, Baker MB, Hecht R, Winters D, Boone T, Collins F. Effects of the obese gene product on body weight regulation in ob/ob mice. Science. 1995; 269(5223):540–543. [PubMed: 7624776]

Sakurai T, Nagata R, Yamanaka A, Kawamura H, Tsujino N, Muraki Y, Kageyama H, Kunita S, Takahashi S, Goto K, Koyama Y, Shioda S, Yanagisawa M. Input of orexin/hypocretin neurons revealed by a genetically encoded tracer in mice. Neuron. 2005; 46(2):297–308. [PubMed: 15848807]

Saper CB, Chou TC, Elmquist JK. The need to feed: homeostatic and hedonic control of eating. Neuron. 2002; 36(2):199–211. [PubMed: 12383777]

Schwartz MW, Woods SC, Porte D Jr, Seeley RJ, Baskin DG. Central nervous system control of food intake. Nature. 2000; 404(6778):661–671. [PubMed: 10766253]

Schüz A, Chaimow D, Liewald D, Dortenman M. Quantitative aspects of corticocortical connections: a tracer study in the mouse. Cereb Cortex. 2006; 16(10):1474–1486. [PubMed: 16357338]

Scott M, Lachey J, Sternson S, Lee C, Elias C, Friedman J, Elmquist J. Leptin targets in the mouse brain. J Comp Neurol. 2008; 514(5):518–532. [PubMed: 19350671]

Ter Horst GJ, Luiten GM. The projections of the dorsomedial hypothalamic nucleus in the rat. Brain Res Bull. 1986; 16:231–248. [PubMed: 3697791]

Thompson RH, Canteras NS, Swanson LW. Organization of projections from the dorsomedial nucleus of the hypothalamus: a PHA-L study in the rat. J Comp Neurol. 1996; 376(1):143–173. [PubMed: 8946289]

van de Wall E, Leshan R, Xu AW, Balthasar N, Coppari R, Liu SM, Jo YH, MacKenzie RG, Allison DB, Dun NJ, Elmquist J, Lowell BB, Barsh GS, de Luca C, Myers MG Jr, Schwartz GJ, Chua SC Jr. Collective and individual functions of leptin receptor modulated neurons controlling metabolism and ingestion. Endocrinology. 2008; 149(4):1773–1785. [PubMed: 18162515]

Yang L, Scott KA, Hyun J, Tamashiro KL, Tray N, Moran TH, Bi S. Role of dorsomedial hypothalamic neuropeptide Y in modulating food intake and energy balance. J Neurosci. 2009; 29(1):179–190. [PubMed: 19129396]

Yoshida K, Li X, Cano G, Lazarus M, Saper C. Parallel Preoptic Pathways for Thermoregulation. J Neurosci. 2009; 29(38):11954–11964. [PubMed: 19776281]

Zigman JM, Nakano Y, Coppari R, Balthasar N, Marcus JN, Lee CE, Jones JE, Deysher AE, Waxman AR, White RD, Williams TD, Lachey JL, Seeley RJ, Lowell BB, Elmquist JK. Mice lacking ghrelin receptors resist the development of diet-induced obesity. J Clin Invest. 2005; 115(12): 3564–3572. [PubMed: 16322794]

Zolotukhin S, Byrne BJ, Mason E, Zolotukhin I, Potter M, Chesnut K, Summerford C, Samulski RJ, Muzyczka N. Recombinant adeno-associated virus purification using novel methods improves infectious titer and yield. Gene Ther. 1999; 6(6):973–985. [PubMed: 10455399]

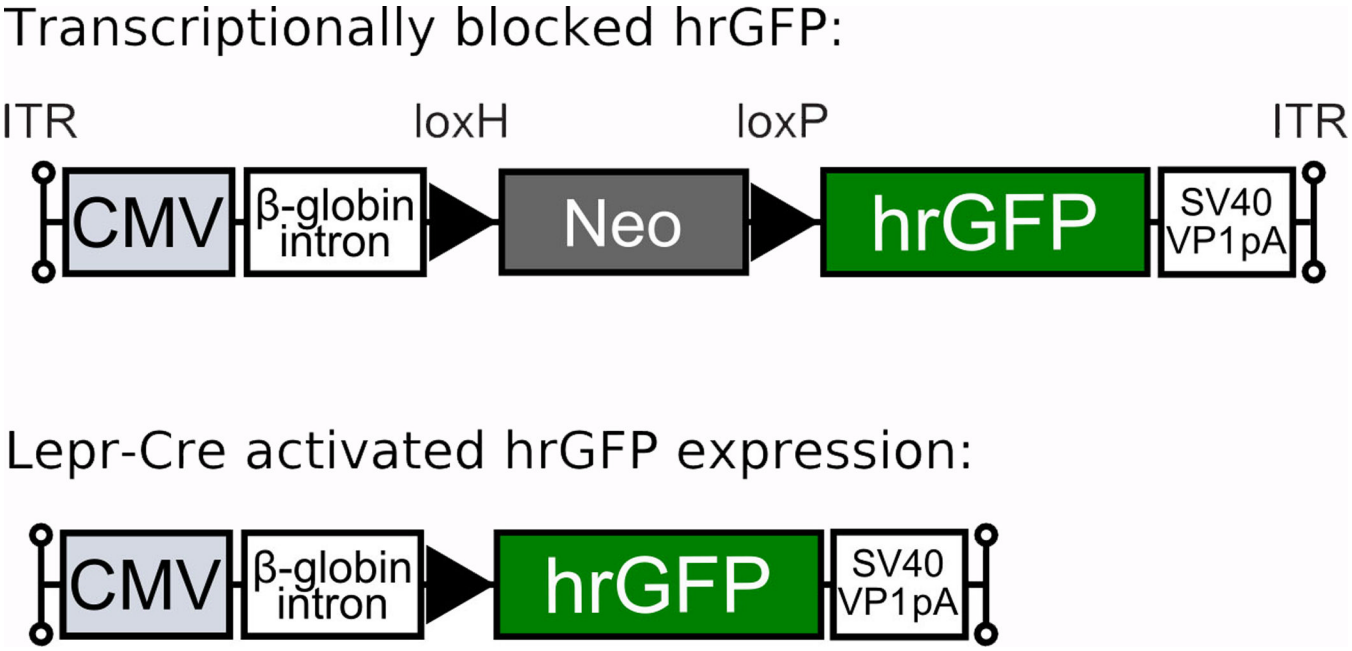

Figure 1.

Generation of a conditional hrGFP-expressing AAV vector. A loxH/loxP-flanked Neo DNA sequence was inserted to prevent transcription of the hrGFP gene. The AAV-lox-Stop-hrGFP cassette consists of a variety of elements in the following order (5' to 3'): left inverted terminal repeat (ITR) - cytomegalovirus (CMV) immediate early promoter – human β-globin intron – loxH site – Neo^R coding sequence – loxP site – hrGFP coding sequence – SV40 VP1 poly A – right ITR. The Cre-mediated removal of the Neo-Stop sequence enables the expression of hrGFP.

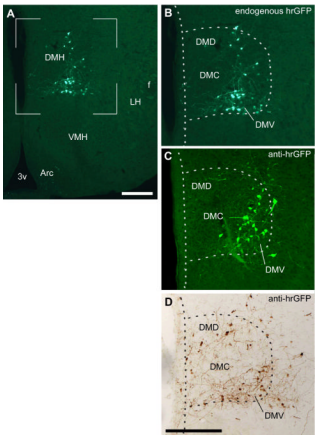

Figure 2.

Expression of hrGFP in one successful injection of AAV-stop-lox-hrGFP (case #5). Endogenous fluorescence (epifluorescence illumination) is observed in many cells in the DMH but not the surrounding structures (A). Higher magnification shows that hrGFP-positive neurons are located mostly in the DMV (B). Fluorescently-labeled adjacent section (epifluorescence illumination and Apotome) (C) and DAB-labeled adjacent section (brightfield illumination) (D) revealed a comparable expression of hrGFP, with a somewhat larger number of cells and fibers. The dotted outline shows the boundary of the DMH. Abbreviations: 3v, third ventricle; Arc, arcuate nucleus of the hypothalamus; DMD, dorsal part of the dorsomedial nucleus of the hypothalamus; DMV, ventral part of the dorsomedial nucleus of the hypothalamus; DMC, compact part of the dorsomedial nucleus of the hypothalamus; f, fornix; LH, lateral hypothalamus; VMH, ventromedial nucleus of the hypothalamus. Scale bars: A=134 μm; B–D; 200 μm.

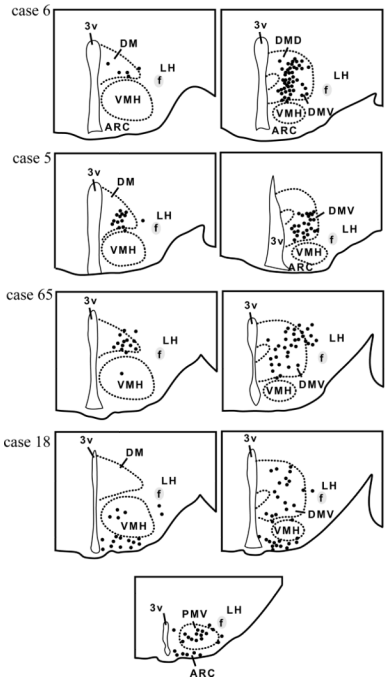

Figure 3.

Camera lucida drawings of 2 rostral-to-caudal levels of the mouse hypothalamus illustrate the distribution of hrGFP-positive cells in 4 successful cases (LepRb-Cre mice). Each dot represents one positive neuron. Note that positive neurons are mostly restricted to the DMH in cases 5, 6 and 65, whereas hrGFP expression was observed outside of the DMH in case 18. Abbreviations: 3v, third ventricle; Arc, arcuate nucleus of the hypothalamus; DM, rostral part of the dorsomedial nucleus of the hypothalamus; DMD, dorsal part of the dorsomedial nucleus of the hypothalamus; DMV, ventral part of the dorsomedial nucleus of the hypothalamus; f, fornix; LH, lateral hypothalamus; PMV, ventral premammillary nucleus; VMH, ventromedial nucleus of the hypothalamus.

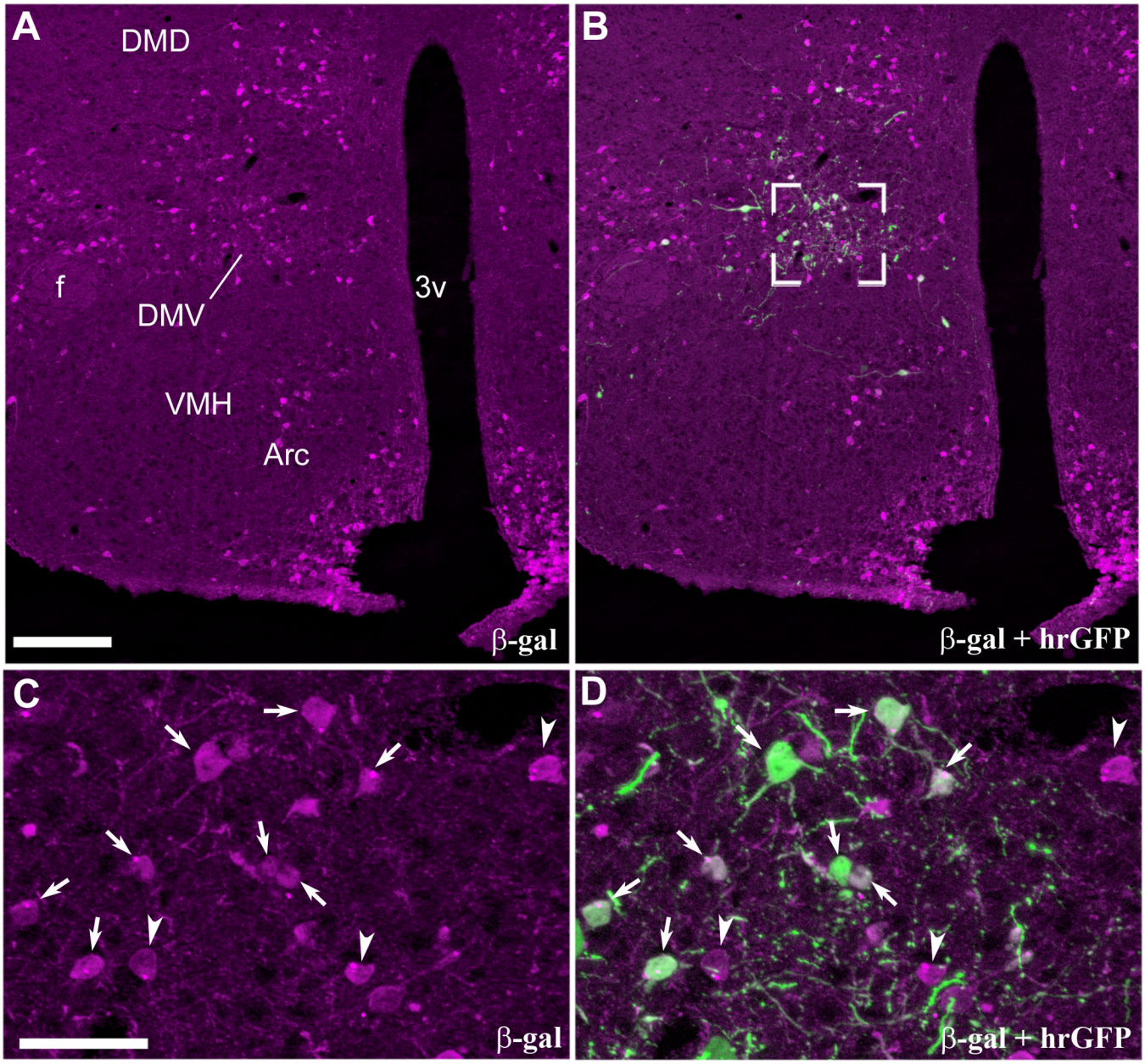

Figure 4.

Restricted expression of hrGFP in leptin-responsive neurons as demonstrated by dual-label immunohistochemistry (case #4, LepRb-Cre-LacZ). Robust β-gal immunoreactivity (Alexa 594) is seen in leptin-responsive neurons distributed in the hypothalamus (A). By contrast, hrGFP-positive neurons (Alexa 488) are observed only in the DMH ipsilateral to the site of injection (B). High magnification photomicrographs reveal clusters of β-gal-positive neurons in the DMV (C). Dual-label labeling showing that hrGFP immunoreactivity coincided perfectly with β-gal (D). It shows that all hrGFP-positive neurons are also leptin-responsive neurons (arrows indicate colocalizations). However, some neurons positive for β-gal do not express hrGFP (arrowheads). Images have been converted to magenta-green. Scale bar in A applies to B, and scale bar in C applies to D. Abbreviations: 3v, third ventricle; Arc, arcuate nucleus of the hypothalamus; DMD, dorsal part of the dorsomedial

nucleus of the hypothalamus; DMV, ventral part of the dorsomedial nucleus of the hypothalamus; f, fornix; VMH, ventromedial nucleus of the hypothalamus. Scale bars: A–B=200μm; C–D=50μm.

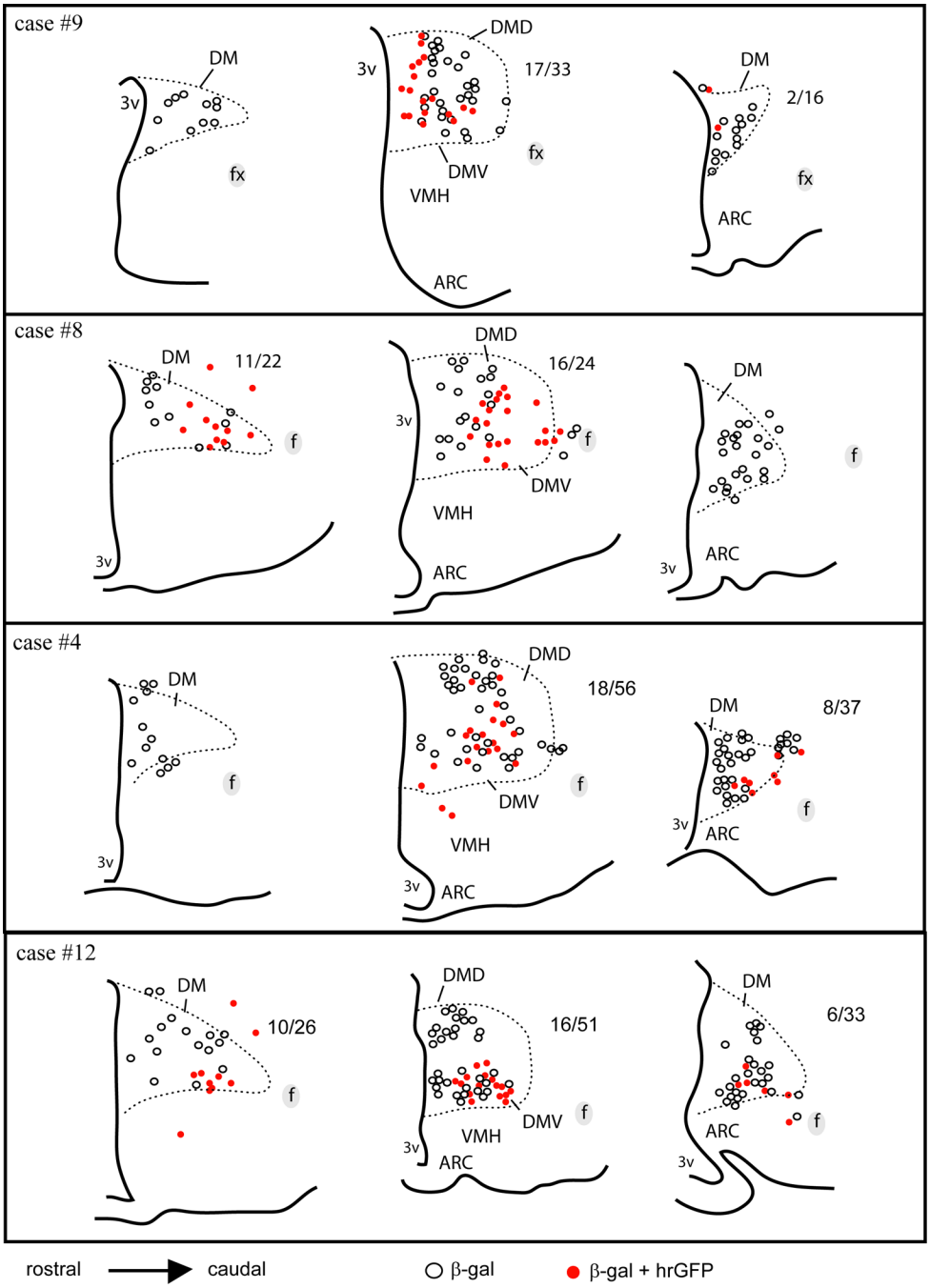

Figure 5.

Camera lucida drawings of 3 rostral-to-caudal levels of the mouse hypothalamus illustrate the distribution of cells positive for β-gal alone (white dots) or β-gal and hrGFP (red dots) in 4 successful cases (LepRb-Cre-LacZ mice). Each dot represents one positive neuron. The ratio of cells positive for hrGFP over the total number of β-gal-positive neurons is indicated next to each brain section (except when no colocalization was observed). Note that the number of hrGFP-positive neurons is more important in the ventral part of the medial DMH in all cases, whereas it considerably varies in the rostral and posterior DMH. Abbreviations: 3v, third ventricle; Arc, arcuate nucleus of the hypothalamus; DM, rostral part of the dorsomedial nucleus of the hypothalamus; DMD, dorsal part of the dorsomedial nucleus of

the hypothalamus; DMV, ventral part of the dorsomedial nucleus of the hypothalamus; f, fornix; VMH, ventromedial nucleus of the hypothalamus.

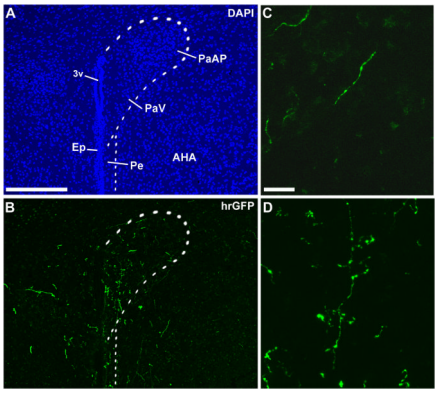

Figure 6.

Immunohistochemical labeling of hrGFP-positive axonal projections in the PVH (A, B). Fibers positive for hrGFP were seen coursing toward the PVH (C), and clusters of terminals were found in the PVH itself (D). Note that fibers were more abundant on the side ipsilateral to the site of injection. The dotted outline shows the boundary of the PVH. Scale bar in A applies to B, and scale bar in C applies to D. Abbreviations: 3v, third ventricle; AHA, anterior hypothalamic area; Ep, ependyma; PaAP, anterior part of the paraventricular nucleus of the hypothalamus; PaV, ventral part of the paraventricular nucleus of the hypothalamus; Pe, periventricular hypothalamic nucleus. Scale bars: A–B=200μm; C–D=20μm.

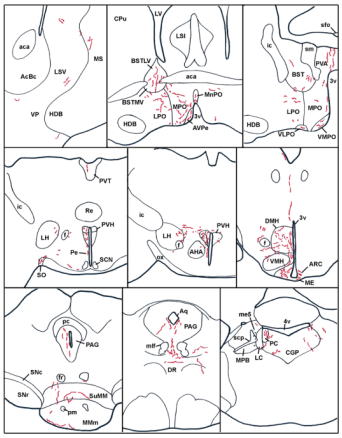

Figure 7.

Anatomical distribution of hrGFP-positive fibers in the brain of case #65 (LepRb-Cre). Abbreviations: 3v, third ventricle; 4v, fourth ventricle; aca, anterior commissure; AcBc, core of the accumbens nucleus; AHA, anterior hypothalamic area; Aq, aqueduct; Arc, arcuate nucleus of the hypothalamus; AVPe, anteroventral periventricular nucleus; BST, bed nucleus of the stria terminalis; BSTLV, lateroventral part of the bed nucleus of the stria terminalis; BSTMV, medioventral part of the bed nucleus of the stria terminalis; CGP; central gray of the pons; CPu, caudate putamen; DMH, dorsomedial nucleus of the hypothalamus; DR, dorsal raphé; f, fornix; fr, fasciculus retroflexus; HDB, nucleus of the horizontal limb of the diagonal band; ic, internal capsule; LH, lateral hypothalamus; LC, Locus coeruleus; LPO, lateral preoptic area; LSi, intermediate part of the lateral septal nucleus; LSV, ventral part of the lateral septal nucleus; LV, lateral ventricle; ME, median eminence; me5, mesencephalic trigeminal nucleus; MMm, median part of the medial mammillary nucleus; MnPO, Median preoptic nucleus; mlf, medial longitudinal fasciculus; MPB, medial parabrachial nucleus; MPO, medial preoptic nucleus; MS, medial septal nucleus; ox, optic chiasm; PAG, periaqueductal gray; PC, precoeruleus; Pe, periventricular hypothalamic nucleus; pm, principal mammillary tract; PVA, anterior part of the paraventricular thalamic nucleus; PVH, paraventricular nucleus of the hypothalamus; PVT; periventricular thalamus; Re, reunions thalamic nucleus; SCN, suprachiasmatic nucleus; scp, superior cerebellar peduncle; sfo, subfornical organ; sm, stria medullaris of the thalamus; SNc, compact part of the subtantia nigra; SNr, reticular part of the subtantia nigra; SO, supraoptic nucleus; suMM, median part of the supramedial mammillary nucleus; VLPO, ventrolateral preoptic area; VMH, ventromedial nucleus of the hypothalamus; VMPO, ventromedial preoptic area; VP, ventral pallidum.

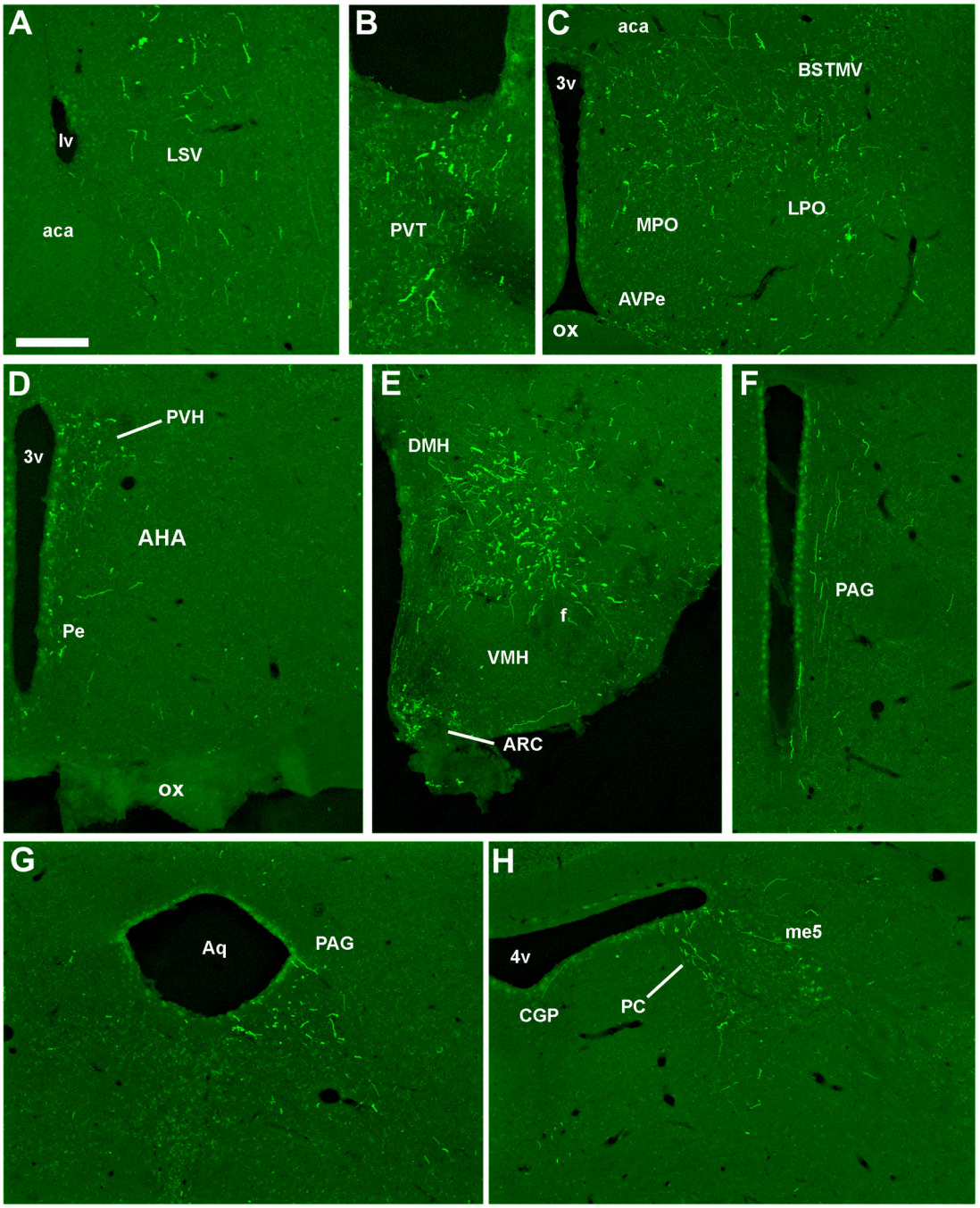

Figure 8.

Photomicrographs of hrGFP-positive fibers in representative structures from case #8 (LepRb-Cre-LacZ) including the LSV (A), PVT (B), BST (C), PVH (D), Arc and DMH (E), PAG (F, G), PC (H). Abbreviations: 3v, third ventricle; 4v, fourth ventricle; aca, anterior commissure; AHA, anterior hypothalamic area; Aq, aqueduct; Arc, arcuate nucleus of the hypothalamus; AVPe, anteroventral periventricular nucleus; BSTMV, medioventral part of the bed nucleus of the stria terminalis; CGP; central gray of the pons; DMH, dorsomedial nucleus of the hypothalamus; LPO, lateral preoptic area; LSV, ventral part of the lateral septal nucleus; LV, lateral ventricle; me5, mesencephalic trigeminal nucleus; MPO, medial preoptic nucleus; ox, optic chiasm; PAG, periaqueductal gray; PC, precoeruleus; Pe,

periventricular hypothalamic nucleus; PVH, paraventricular nucleus of the hypothalamus; PVT; periventricular thalamus; VMH, ventromedial nucleus of the hypothalamus. Scale bar: A–H=200 μm.

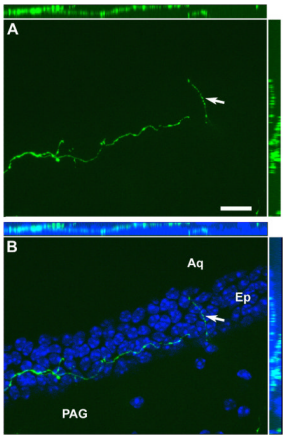

Figure 9.

Optical sections reconstruction (epifluorescence and Apotome) of a hrGFP-positive fiber (A) demonstrating that it is traveling inside the ependymal layer in all 3 dimensions (B). The ependymal layer of the aqueduct is revealed by DAPI staining (B). The white arrow shows an axonal branch running through the ependyma. Scale bar in A applies to B. Abbreviations: Aq, aqueduct; Ep, ependymal layer; PAG, periaqueductal gray. Scale bar: A–B= 200μm.

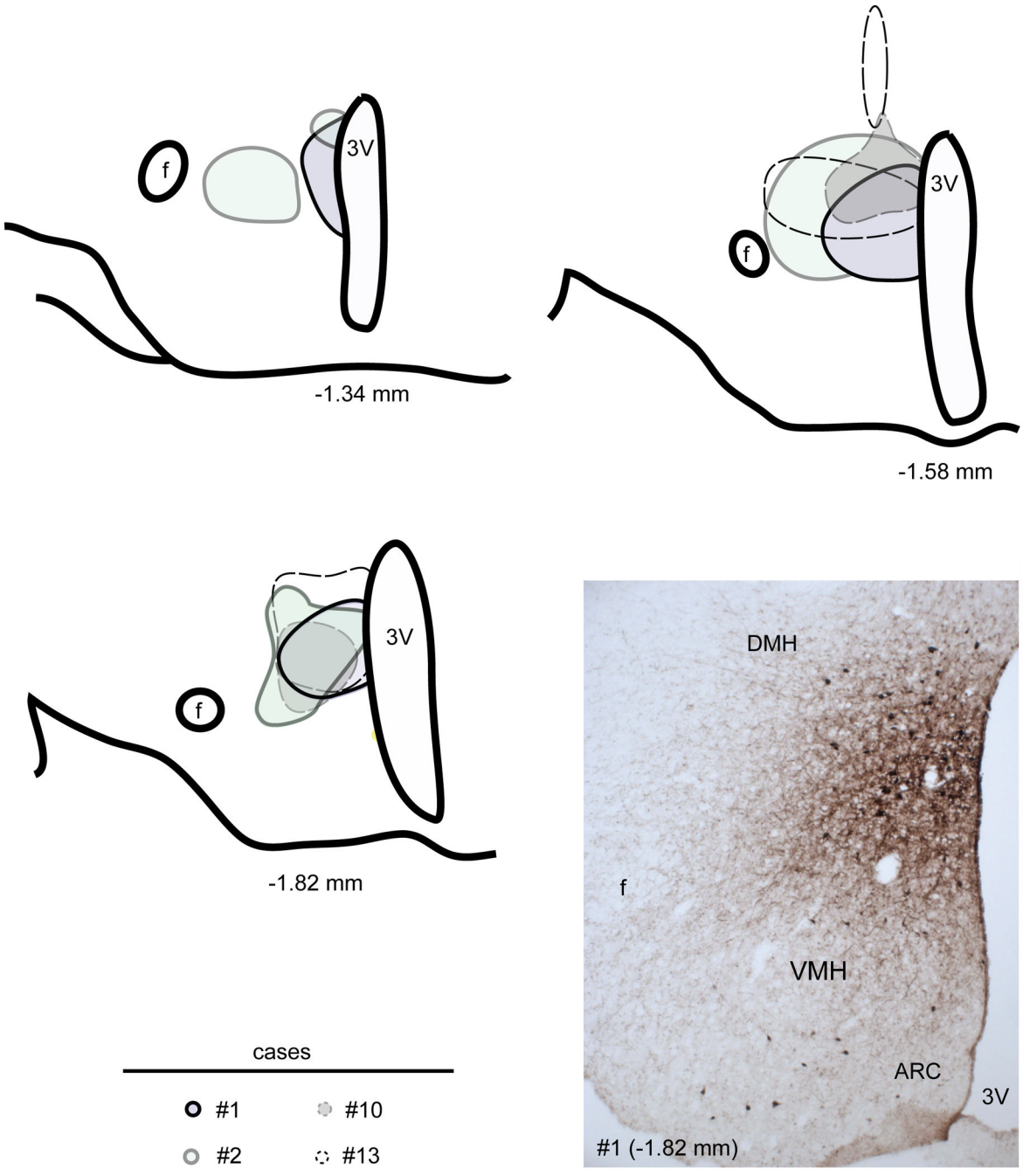

Figure 10.

Camera lucida drawings of 3 rostral-to-caudal levels of the mouse hypothalamus illustrate the distribution of BDA deposits in 4 successful cases (distance from bregma is indicated below each level). Sites of injections are circled. A photomicrograph from case #1 appears in the bottom right panel. Abbreviations: 3v, third ventricle; Arc, arcuate nucleus of the hypothalamus; DMH, dorsomedial nucleus of the hypothalamus; VMH, ventromedial nucleus of the hypothalamus; f, fornix.

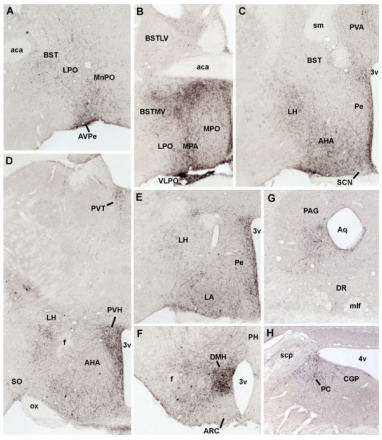

Figure 11.

Photomicrographs of BDA-positive fibers in representative structures from case #1. Abbreviations: 3v, third ventricle; 4v, fourth ventricle; aca, anterior commissure; AHA, anterior hypothalamic area; Aq, aqueduct; Arc, arcuate nucleus of the hypothalamus; AVPe, anteroventral periventricular nucleus; BST, bed nucleus of the stria terminalis; BSTLV, lateroventral part of the bed nucleus of the stria terminalis; BSTMV, medioventral part of the bed nucleus of the stria terminalis; CGP; central gray of the pons; DMH, dorsomedial nucleus of the hypothalamus; DR, dorsal raphé; f, fornix; LH, lateral hypothalamus; LPO, lateral preoptic area; MnPO, Median preoptic nucleus; mlf, medial longitudinal fasciculus; MPB, medial parabrachial nucleus; MPA, medial preoptic area; MPO, medial preoptic nucleus; ox, optic chiasm; PAG, periaqueductal gray; PC, precoeruleus; Pe, periventricular hypothalamic nucleus; PH, posterior hypothalamus; PVA, anterior part of the paraventricular thalamic nucleus; PVH, paraventricular nucleus of the hypothalamus; PVT; periventricular thalamus; SCN, suprachiasmatic nucleus; scp, superior cerebellar peduncle; sm, stria medullaris of the thalamus; SO, supraoptic nucleus; VLPO, ventrolateral preoptic area; VMH, ventromedial nucleus of the hypothalamus; VMPO, ventromedial preoptic area.

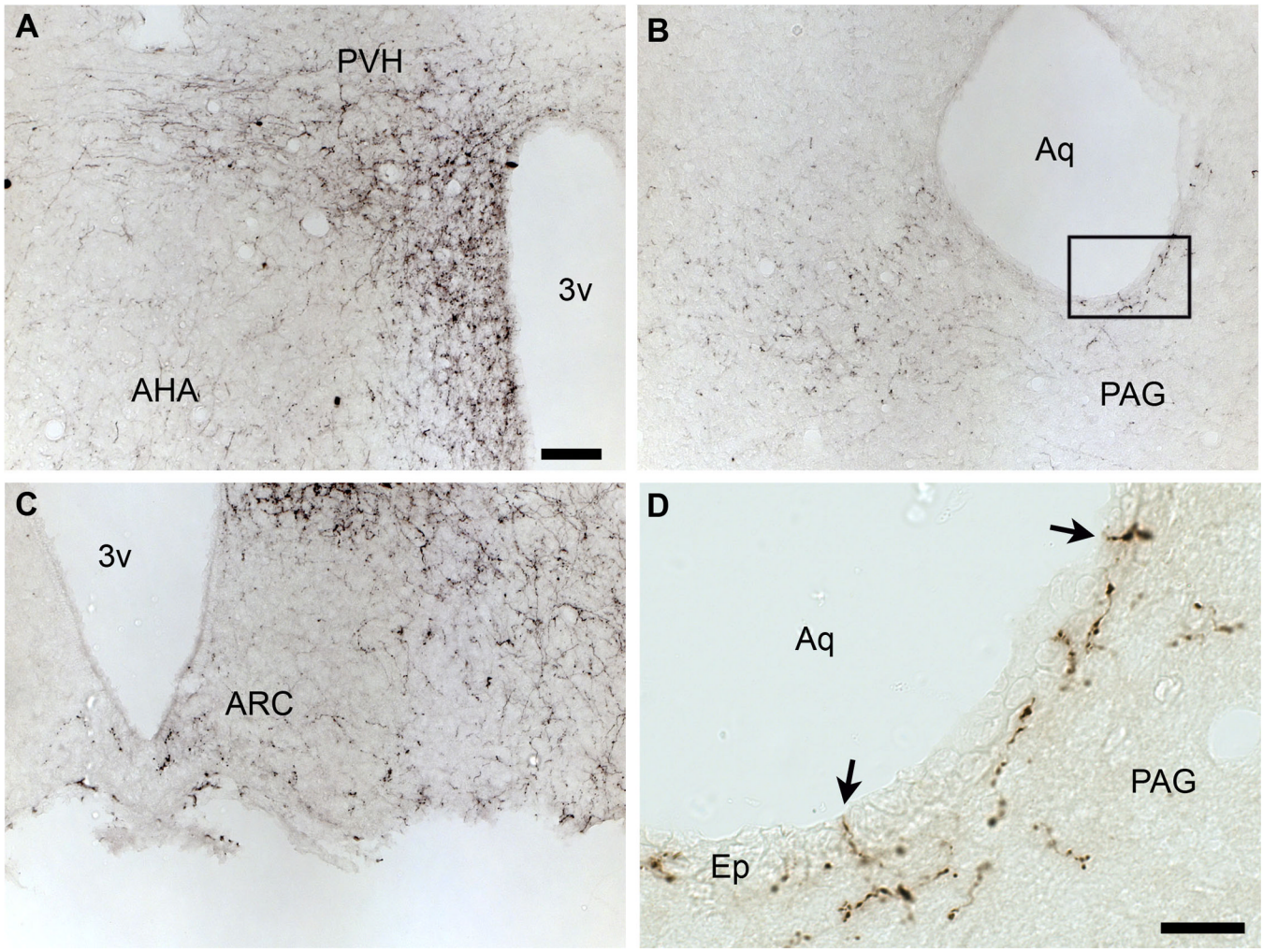

Figure 12.

Immunohistochemical labeling of BDA-positive axonal projections in the PVH (A), PAG (B, D) and Arc (C). Note the fibers traveling closely to the ventricle near the PAG (B). At high magnification, it appears that some fibers travel through the ependymal layer itself (arrows) (D). Abbreviations: 3v, third ventricle; Arc, Arcuate nucleus; AHA, anterior hypothalamic area; Ep, ependyma; PVH, paraventricular nucleus of the hypothalamus; PAG, periaqueductal gray. Scale bar: A–C= 50μm; D= 20μm.

Table 1

Primary antisera.

Antigen	Immunogen	Manufacturer	Dilution used
hrGFP	Full length recombinant hrGFP from E.Coli	Stratagene, Cat. # 240142-51, lot0830269	1:30,000 and 1:50,000
β-galactosidase	Full length purified β-galactosidase from E.Coli	Abcam, Cambridge, MA; Cat. # ab9361-250, lot397981	1:4,000

Table 2

Relative densities of hrGFP-positive fibers and BDA-positive fibers originating from leptin sensitive DMH neurons and generic DMH neurons respectively.

Structures	hrGFP-IR (cases #6, 5, 65, 9, 8, 4, 12)	BDA-IR (cases #1, 2, 10, 13)
LSV	+	+ +
MS	+/−	+
VP	+/−	+
BSTLV	+	+ +
BSTMV	+	+ +
BST	+	+
LPO	+	+ +
MPA	+	+ + + +
MPO	+	+ + +
MnPO	+/−	+ +
AVPe	+	+ + +
VLPO	+	+ + +
VMPO	+	+ + +
PVA	+	+ +
PVT	+	+ +
Pe	+ +	+ + +
LH	+	+ +
SO	+/−	+
AHA	+/−	+ +
PVH	+ +	+ + + +
DMH	+ +	+ + + +
Arc	+ +	+
PH	+	+ +
MMm	+	+ +
SuMM	+	+ +
PAG	+	+ +
DR	+/−	+
RP	−	+/−
PC	+	+ +
CGP	+/−	+

+ + + +, very high; + + +, high; + +, moderate; +, low; +/−; not consistently seen; −, absent.

Abbreviations: AHA, anterior hypothalamic area; Arc, arcuate nucleus of the hypothalamus; AVPe, anteroventral periventricular nucleus; BST, bed nucleus of the stria terminalis; BSTLV, lateroventral part of the bed nucleus of the stria terminalis; BSTMV, medioventral part of the bed nucleus of the stria terminalis; CGP; central gray of the pons; DMH, dorsomedial nucleus of the hypothalamus; DR, dorsal raphé; LH, lateral hypothalamus; LPO, lateral preoptic area; LSV, ventral part of the lateral septal nucleus; MnPO, Median preoptic nucleus; MPA, medial preoptic area; MPO, medial preoptic nucleus; MS, medial septal nucleus; PAG, periaqueductal gray; PC, precoeruleus; Pe, periventricular hypothalamic nucleus; PH, posterior hypothalamus; PVA, anterior part of the paraventricular thalamic nucleus; PVH, paraventricular nucleus of the hypothalamus; PVT; periventricular thalamus; RP, raphe pallidus; SO, supraoptic nucleus; VLPO, ventrolateral preoptic area; VMPO, ventromedial preoptic area; VP; ventral pallidum